

# Influence of Flood Conditions and Vegetation Status on the Radar Backscatter of Wetland Ecosystems

by P. Kandus • H. Karszenbaum • T. Pultz • G. Parmuchi • J. Bava

## RÉSUMÉ

L'objectif de cet article est d'évaluer l'utilisation des données RSO de RADARSAT pour l'identification des écosystèmes de terres humides prenant en considération l'influence des caractéristiques des cibles (type de végétation, conditions d'inondation, phénologie et les feux), ainsi que les paramètres du capteur (angles d'incidence variables). Les îles du delta inférieur du fleuve Paraná en Argentine ont été choisies comme zone d'étude. Six images RSO acquises au cours de l'été et de l'hiver 1997 et 1998 ont été utilisées. Cet ensemble fait appel aux modes standard S1, S4 et S6 pour tenir compte des effets d'angle d'incidence. Les valeurs de rétrodiffusion radar d'échantillons prélevés sur des sites connus ont été analysées. Le signal de rétrodiffusion de la forêt montre une stabilité temporelle au cours de l'été et de l'hiver, que ce soit en présence ou en absence de feuilles dans les arbres. Au contraire, la rétrodiffusion de la forêt est fortement mise en valeur par la présence d'eau sous-jacente. On a trouvé que les retours radar pouvaient varier d'un signal atténué à un signal caractérisé par un comportement de type double rebond. Dans les terres humides dominées par les joncs, le mécanisme dominant d'interaction peut varier d'une réflexion de type double rebond à une réflexion de type spéculaire dû aux inondations. Dans des conditions de niveau normal des eaux, on a pu déterminer que la capacité de différencier la forêt de la végétation herbacée diminue en fonction de l'accroissement de l'angle d'incidence. Dans des conditions extrêmes d'inondation, la rétrodiffusion radar diminue en fonction de l'accroissement de l'angle d'incidence, d'environ 3 dB pour la forêt et de 4 dB pour les joncs.

## SUMMARY

The aim of this paper is to assess the use of RADARSAT SAR data for wetland ecosystem identification considering the influence of target features (vegetation type, flood conditions, phenology, and fires), as well as sensor parameters (varying incidence angles). The Lower Delta islands of the Paraná River in Argentina were selected as the study area. Six SAR images acquired during the summer and winter of 1997 and 1998 were used. This set includes Standard Beams S1, S4 and S6 to account for the incidence angle effect. Radar backscatter of samples taken at known sites was analyzed. The forest backscatter signal shows temporal stability during summer and winter, either with leaf-on or leaf-off trees. On the contrary, backscattering from forest is strongly enhanced by underlying water. Radar returns were found to change from an attenuated signal to one dominated by double-bounce behaviour. In wetlands dominated by rushes, the dominant interaction mechanism may change from double-bounce to specular reflection due to flood. During normal water-level conditions, the ability to differentiate forest from herbaceous vegetation was found to decrease with increasing incidence angle. Under extreme flooding, radar backscattering decreases from steep to shallow incidence angles, about 3 dB for forest, and 4 dB for rushes.

Manuscript received: July 14, 2000 / Revised: June 4, 2001.

• P. Kandus is with Laboratorio de Ecología Regional, Departamento de Biología - Facultad de Ciencias Exactas y Naturales, Universidad de Buenos Aires (UBA) Ciudad Universitaria, Pab. II 4to.piso. (1428) Buenos Aires, Argentina. E-mail: pato@bg.fcen.uba.ar.

• H. Karszenbaum, G. Parmuchi and J. Bava are with CONICET - Instituto de Astronomía y Física del Espacio (IAFE), Pabellón IAFE, Ciudad Universitaria (1428), Buenos Aires, Argentina. E-mail: haydeek@iafe.uba.ar.

• T. Pultz is with the Applications Division, Canada Centre for Remote Sensing, 588 Booth Street, Ottawa, Canada. E-mail: Terry.Pultz@CCRS.NRC.ca.

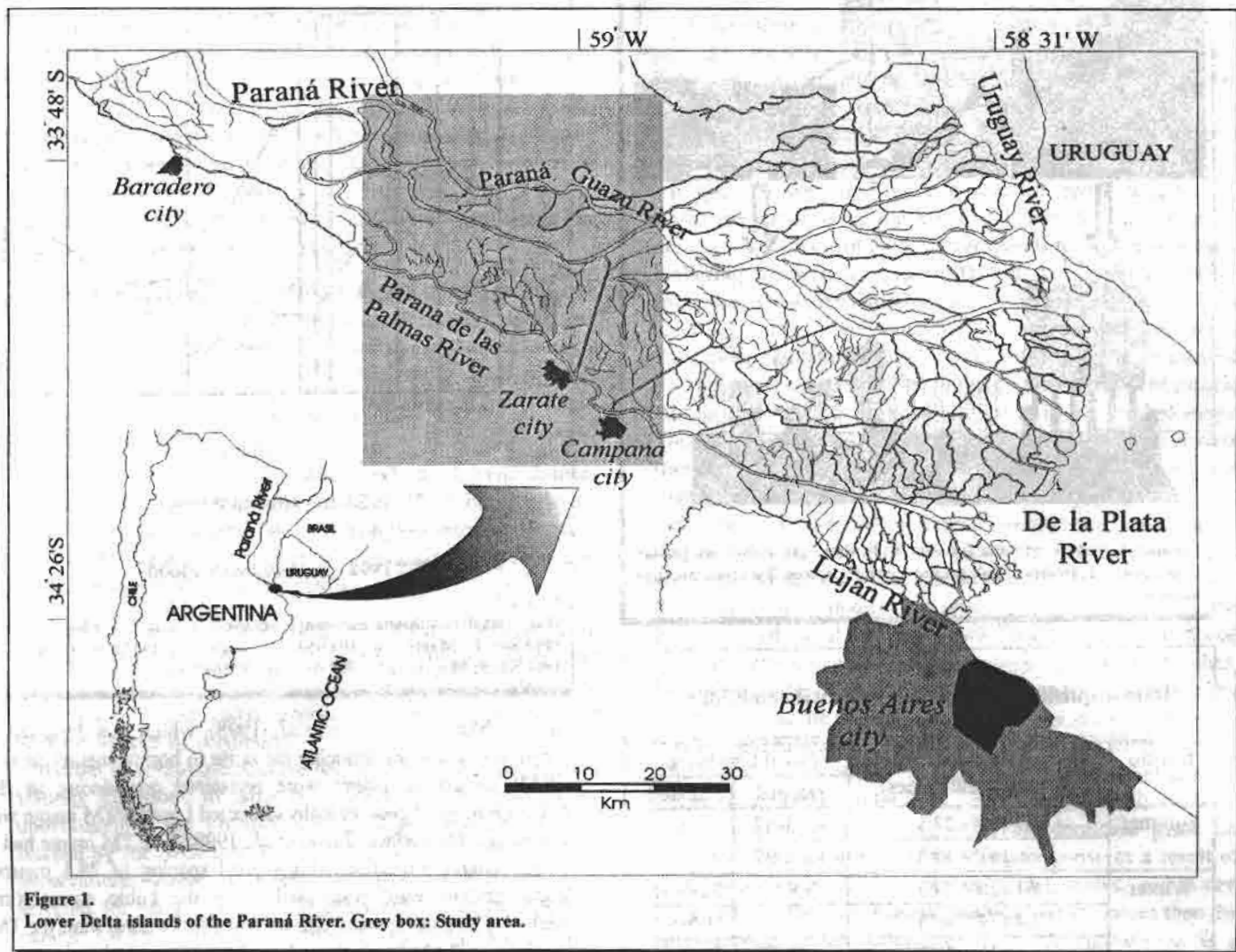


Figure 1.  
Lower Delta islands of the Paraná River. Grey box: Study area.

increase in water level from September to March with a minimum around August. Extraordinary inundation events can also be triggered by El Niño phenomena, such as that of 1998.

Figure 2 schematically shows the main land cover types of the study area. Lowlands cover around 42 percent of the area and are characterized by rush plant communities mainly dominated by *Schaenoplectus californicus* (Kandus, 1997). This species is a perennial equisetoid up to 2.5 metres high presenting around 80 percent of ground coverage. Across the lowlands, there are thin meander belts covered by prairies with herbaceous and woody plants strongly degraded by cattle grazing. About 40 percent of the original natural vegetation of the area was completely replaced by human activities mainly represented by willow (*Salix* spp.) and poplar (*Populus* spp.) plantations. Salicaceae species are all deciduous, and leafless from late April to September. In order to plant and manage forest plantations, logging and sometimes burning of the existing vegetation are required. In some cases, soil drainage is enhanced by channels that speed up water outflow. In other cases, polders prevent water input from river floods. Fires are also frequent in the region, adding variability and creating

confusion when remote sensing images are analyzed. The entire area is affected by forcing factors such as precipitation and winds, flood conditions, and phenology.

#### Data Description and Preparation

Six Standard Mode RADARSAT images from ascending passes were used for this study. The RADARSAT SAR operates at C-band (5.3 GHz) in HH polarization. The Standard Mode images examined (SGF) have a nominal resolution of 25 metres in range (ground range resolution varies with range), and 28 metres in azimuth, and are processed to four looks (<http://www.ccrs.nrcan.gc.ca/ccrs/tekrd/radarsat/specs/radspece.html>). The main differences between scenes are season, flood condition, and angle of incidence (Table 1). Three of the scenes were acquired in the summer and winter of 1997 under almost normal water level conditions. Two of them, using Standard Beam 1 and Standard Beam 6, were acquired in late summer and the other, Standard Beam 1, in winter. The other three images were acquired in winter 1998 during the flood peak of the Paraná River resulting from the "El Niño" event. These three scenes taken during the month of May correspond to three

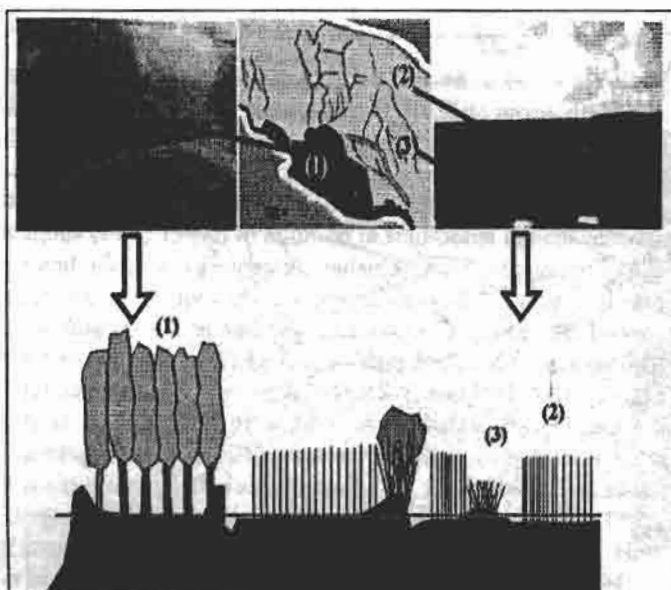


Figure 2. Landscape pattern scheme for the study area. (1) willow or poplar plantations; (2) rushes; (3) degraded meander spires. Blue line: average water level.

Table 1. Data acquisition dates, environmental conditions, and beam modes.

Season	Beams / Incidence Angles (approximate values)	Flood Condition	
		Normal	Flooded
Summer	S1 (20° - 27°)	16-3-97	
	S6 (41° - 46°)	16-2-97	
Winter	S1 (20° - 27°)	7-8-97	22-5-98
	S4 (34° - 40°)		4-5-98
	S6 (41° - 46°)		12-5-98

different incidence angles: Standard Beam 1, Standard Beam 4, and Standard Beam 6. The *Servicio de Construcciones Portuarias y Vías Navegables* contributed monthly mean water level data at the port of Zárate, as well as hourly water levels for the dates of image acquisition. Figure 3 illustrates monthly mean water level during a normal period (average conditions from 1976 to 1980) as well as for the years where images were acquired: 1997 and 1998. Data about winds (intensity and direction) and precipitation for these dates were also available.

In addition to radar images, Landsat 5-Thematic Mapper images provided by the Argentine National Agency for Space Activities (Comisión Nacional de Actividades Espaciales - CONAE) were available, along with panchromatic aerial photographs, field data, and a vegetation map obtained from optical data (Kandus, 1997; Kandus *et al.*, 1999).

Proper assessment of environmental conditions and incidence angle effects require absolute backscattering values. Using PCI software version 6.3, images of the radar backscattering coefficient ( $\sigma^0$ ), expressed in power, were obtained for all scenes. Next, speckle was reduced by image filtering using a 3x3 window

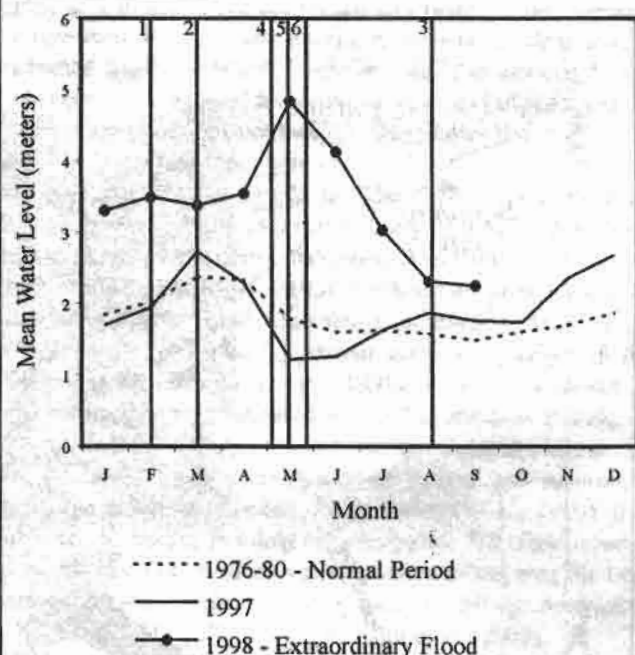


Figure 3. Water level conditions for image acquisition dates. 1: February 16, 1997/S6; 2: March 16, 1997/S1; 3: August 7, 1997/S1; 4: May 1, 1998/S4; 5: May 18, 1998/S6; 6: May 22, 1998/S1.

Gamma Map filter (Frulla *et al.*, 1998), which was designed to preserve edges while reducing the noise in homogeneous areas.

SAR images in power were registered considering as the reference image a geometrically corrected Landsat/TM image and assuming a flat surface (Frulla *et al.*, 1998). The TM image had a Gauss Kruger projection with a pixel spacing of 28.5 metres. Radar images were resampled using the cubic convolution method. The pixel spacing chosen was 14.25 metres (half the TM pixel size, 28.5). Approximately 50 ground control points were used for each image registration task. In average, the RMS error was of the order of 0.50 pixels (Frulla *et al.*, 1998; Milovich *et al.*, 2000). Next, images in amplitude (for visual analysis), and in decibels were calculated from the geolocated  $\sigma^0$  (in power) scenes.

A subset corresponding to the study area was selected from each radiometrically processed and geometrically corrected image. The operational limits chosen for the study area correspond to the intersection of S4 and the other scenes.

### Landscape Elements and Information Extraction from Images

As shown in Figure 2, two main landscape elements are dominant in the study area: lowlands with rushes and willow or poplar plantations in middle slopes, highlands, and areas protected by dikes. These landscape elements strongly differ in their structural and dynamic characteristics. Furthermore, environmental conditions and sensor parameters (angle of incidence) may quantitatively or qualitatively modify the interaction mechanisms between the SAR signal and these surface elements, adding difficulty to radar response interpretation.



**Table 2** summarizes the different environmental conditions of main landscape elements (forest plantations and rushes) in the RADARSAT images analyzed. In the case of forest, they may be flooded, burned and, depending on the season, trees may have their leaves on or off. Rushes are perennial, and they are always flooded but they may be also almost completely covered by water or burned.

**Table 2** addresses the following assumptions regarding the dominant interaction mechanisms:

- Volume scattering is considered the dominant interaction mechanism for trees, resulting in an attenuated signal, but under flooded conditions the contribution of trunk surface interaction increases strongly, producing a significant enhancement of the total backscattering coefficient (Richards, 1987b).
- In rushes under normal water level conditions, double-bounce effects are dominant producing high backscattering values; when covered by water and/or burned, forward scattering is the main mechanism causing a strong reduction in radar signal (Pultz *et al.*, 1997).

Based on the above, it may be inferred that depending on the dominant interaction mechanisms between signal and target, the two landscape elements may be readily identified and classified from radar response, or they may become an obvious source of confusion.

In order to obtain quantitative results, amplitude images were visually examined in order to establish a first criterion for understanding the physical relationships between features imaged by the SAR instrument and the corresponding ground observations. Areas of interest of about 400 pixels were selected for each land cover interactively using the ERDAS version 8.4 image processing system, and the statistics (mean and standard deviation) of their calibrated brightness values (in power) were stored. These values were converted from power to decibels for plotting (Karszenbaum *et al.*, 1998; Frulla *et al.*, 1998). For sample selection, information collected in specific field work and interviews with local people were taken into account. Landscape spatial heterogeneity, and different environmental conditions were carefully considered. In addition to the categories of **Table 2**, forest age was also considered: young (2-year) and adult (13-year) plantations, with tree-heights varying from 5 to 15 metres, and DBH ranging between 6 and 20 cm respectively.

## OBSERVATIONS AND DISCUSSION

### Effect of Environmental Conditions on Radar Backscatter

**Figure 4** shows S1 images addressing three main environmental conditions:

- 1) Summer - normal water level;
- 2) Winter - normal water level; and
- 3) Winter - flooded.











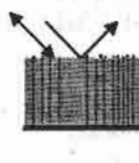

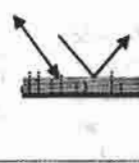

As described in **Figure 2**, the main landscape elements present in the scenes are river water, lowlands with rushes, and Salicaceae afforestations (including willow and poplar plantations). The variations of grey tones are related to structural characteristics of land covers, water content and coherent noise inherent in radar data.

It may be seen in **Figure 4** that the radar response of landscape elements in summer and winter S1 images under normal water level conditions corresponds to similar dominant scattering mechanisms (**Table 2**), but they definitely differ from the S1 winter flooded image. In normal water level condition images, river water shows an intermediate grey tone, Salicaceae plantations appear in dark tones and an enhanced backscattered signal may be easily observed in areas of rushes. Almost opposite grey tones are observed in the flooded scene. The main differences between summer and winter S1 scenes (normal water level conditions) are observed in the area of rushes where important burning occurred in summer.

**Figure 5** shows the measured backscatter values from polygons corresponding to the landscape elements considered, within the S1 scenes. In the case of forest, **Figure 5a** illustrates that leaf on/off conditions introduce slight changes in the backscattered signal showing a difference that does not exceed 2 dB between summer and winter scenes. In the case of rushes, two main clusters may be seen, one corresponding to healthy vegetation, and the other one to areas burned in March. Healthy rushes yield bright returns in both summer and winter scenes. This behaviour is similar to that described by other authors (Hess *et al.*, 1990; Cihlar *et al.*, 1992) for vertically oriented stalks. *Schaenoplectus californicus*, the dominant plant, on saturated soils accounts for the strong response as a result of double-bounce interactions among signal, stalks, and water. Nevertheless, the winter image shows lower  $\sigma^0$  values than the summer one (3 dB difference). Since *S. californicus* is a perennial species and water level and weather conditions are quite similar, no definite explanation for this behaviour has been provided. Additional imagery is necessary to account for this difference. In summer, low backscatter returns correspond to burned rushes. The fire event occurred just before image acquisition: thus, no standing vegetation was present and soil water content caused a strong decrease in radar backscatter (-9dB). In the August scene, rushes had already recovered.

In May 1998, the water level was about two metres above normal and a strong vegetation-water signal interaction is responsible for the large differences in backscatter observed between normal condition and flooded winter images (**Figure 4**). Three main clusters may be seen in **Figure 5b**. One of them corresponds to rushes, another one to flooded forest and the third one to non-flooded forest. In the case of rushes, radar backscatter shows a strong decrease caused by standing water that covers the vegetation. Thus, the main interaction mechanism changed from double-bounce to specular reflection (Dobson *et al.*, 1995). In the case of forest, the behaviour of the non-flooded plantations remains stable. On the other hand, flooded forests show a strong enhancement of radar backscatter (about 10 dB increase). These observations agree well with

**Table 2.**  
**Two main land-cover types, environmental conditions, and dominant scattering mechanisms.**

Land cover type / Condition	Dominant interaction mechanism	General view
forest plantation / non-flooded summer		
forest plantation / non-flooded winter		
forest plantation / non-flooded winter and burned		
forest plantation / flooded summer		
rushes / standing, normal water-level condition		
rushes / flooded		
rushes / burned, normal water-level condition		

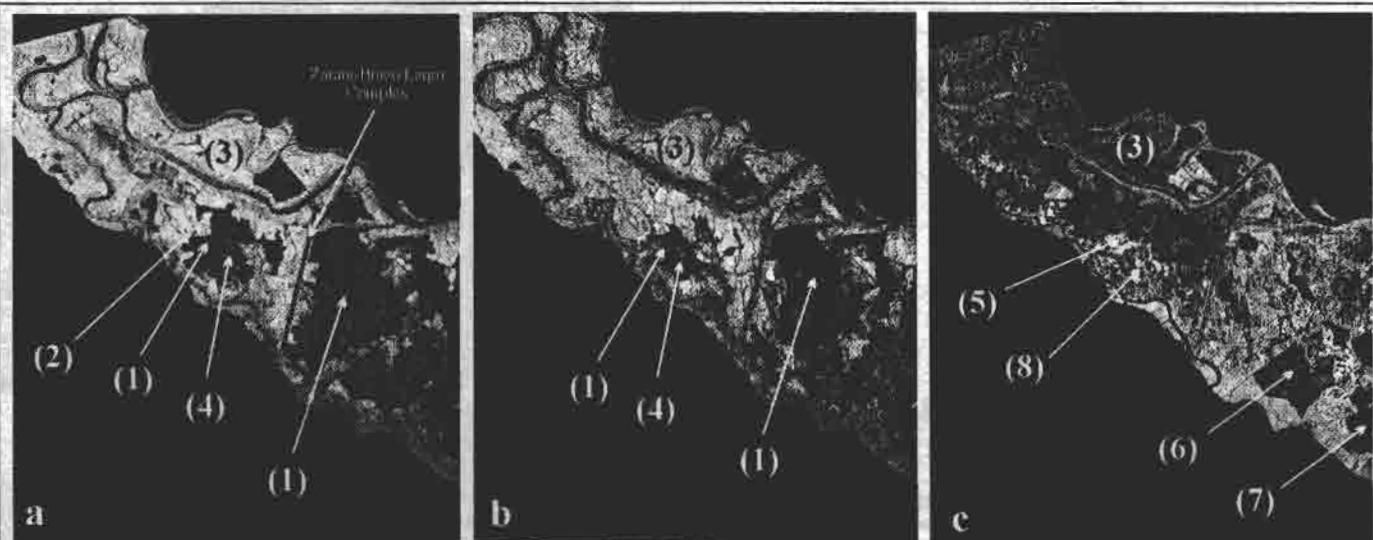


Figure 4. RADARSAT SAR Standard 1 images from: a) March 16, 1997 (late summer); b) August 16, 1997 (winter) and c) May 22, 1998 (winter-flooded). (1) Willow; (2) Burned rushes; (3) Rushes; (4) Burned willow; (5) Flooded willow; (6) Non-flooded poplar; (7) Non-flooded willow; (8) Burned flooded willow.

theoretical predictions provided by canopy backscatter modelling of flooded and non-flooded forest (Richards, 1987b; Crevier and Pultz, 1996; Hess *et al.*, 1995). For flooded areas, the main contribution to radar backscatter changes from volume scattering from the canopy to trunk-water double-bounce interaction.

#### Effect of Beam Mode Incidence Angle on Radar Backscatter

Proper assessment of incidence angle effects demands almost simultaneous, multi-angle calibrated scenes from a single area. In this paper, the effect of incidence angle on landscape element identification has been analyzed under two environmental conditions according to image availability: normal water level condition in summer and flooded condition in winter.

Two single beam mode images have been compared for summer 1997, S1 and S6. As expected, it may be seen that the increase in incidence angle enhances ground-open water boundaries because of a stronger specular reflection effect of smooth water (Figure 6). An opposite effect occurs in vegetated areas. The S6 image shows very subtle differences in the backscatter from forest and rushes in spite of the strong differences in structure. This observation may be explained by the strong attenuation of the wave by aboveground vegetation at higher incidence angles (Figure 7a). The interaction with standing biomass is dominant in the S6 scene. Volume scattering attenuates the signal in most areas and no apparent differences between healthy and burned rushes is observed. However, this is not a uniform behaviour, that is, there are areas of rushes where a corner reflector effect also occurs in the S6 mode (Figure 6). Further field work and imagery are required to understand the complexity of radar returns in the S6 mode for rushes. In general, these observations agree well with the ones described by Kasischke *et al.* (1997a), and by Ribbes *et al.* (1999).

Figures 7b to 7d show the backscattering behaviour of landscape elements under flooded conditions. In the case of rushes there is a decrease in the backscattered signal from S1 to S6. Differences between beams are of the order of 2 dB, and follow a linear trend. When rushes are almost completely covered by water, the signal is specularly reflected away from the sensor and, the larger the incidence angle, the smaller the signal that returns to the sensor. A similar backscattering behaviour occurs for river water, but there is a major difference in intensity between steep and shallow incidence angles (around 10 dB), although the influence of wind on the S1 image cannot be ignored (Pultz *et al.*, 1991; Tandis *et al.*, 1994; Ramsey, 1995; Crevier and Pultz, 1996).

During the 1998 winter flood event, most forest plantations were flooded, but some remained dry. Unfortunately, the S4 image, which covers a smaller area of the Delta (different orbit) than the rest of the images, does not include willow plantations not affected by flood. Consequently, no samples of this category are available for S4. Forest radar backscatter shows a lower return with increasing incidence angle when flooded, and an almost uniform response when the forest floor remains dry during the image sequence (Figures 7b-d). For flooded willow forests, an enhanced backscatter signal is observed in S1, which decreases in S4 and remains almost unchanged in S6 with respect to S4.

Figure 8 shows a multi-angle colour composite image generated from RADARSAT imagery collected during the flood peak of 1998 (Table 1). The S4 image is displayed in red, S6 in green, and S1 in blue. The cyan colour corresponds to areas of a lower return in the S4 image. These are willow plantations that probably were flooded by the end of May (in the case of S1 and S6 images), but were not yet flooded on May 1<sup>st</sup>, when the S4 image was acquired. The bright-white areas correspond to willow plantations flooded during the three acquisition dates. Non-flooded poplar plantations are shown in green. River water is represented in deep blue and areas of rushes present a gradient



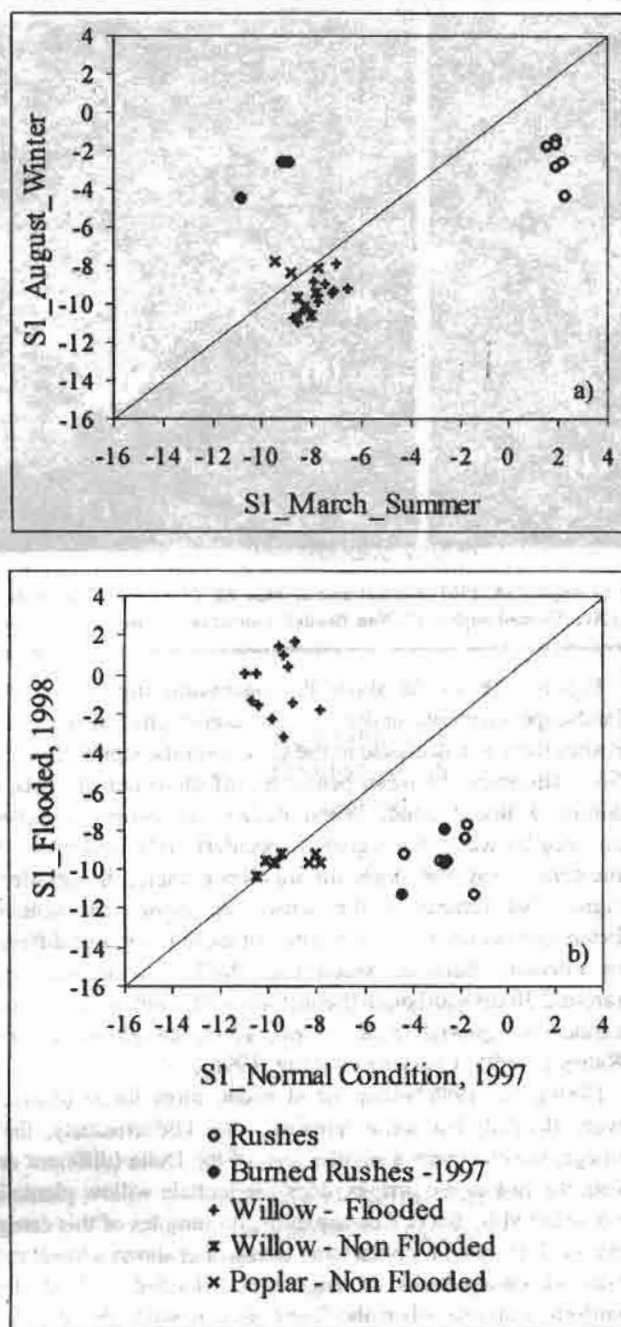


Figure 5. Scatterplots of measured RADARSAT SAR backscatter values from polygons of two main landscape elements under different environmental conditions. a) winter vs. summer; b) flooded vs. normal condition in winter.

from deep blue to reddish-brown indicating spatial heterogeneity. The brighter red corresponds to areas inside dikes with no standing vegetation (clearcut forest or burned rushes). Finally, a complex mosaic of colours corresponds to burned areas within forest plantations. Some burned stands appear as bright as those that were not burned, and others look like the non-flooded forests even though they were flooded. In general, burned areas introduce great confusion in land cover assessment.

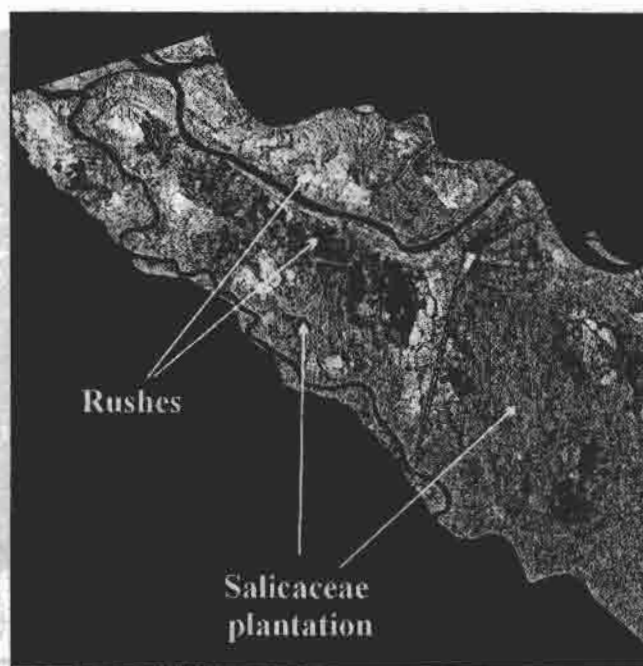


Figure 6. RADARSAT SAR Standard 6 image from February 16, 1999 (late summer).

### Multi-Temporal Multi-Angular Comparison

Figure 9 shows the radar response behaviour of selected samples for each landscape element, and indicates the mean and standard deviation of backscatter values for all images involved in the analysis. Figure 9a clearly shows the importance of the incidence angle for radar return from water. Differences between beams may reach values of the order of 18 dB. Nevertheless, wind conditions cannot be ignored in the S1 scenes.

In the case of rushes, radar backscatter is strongly affected not only by the incidence angle effect but also by changes in environmental conditions (flood and burns) (Figure 9a) that determine the dominant signal vegetation-water interaction mechanisms. For healthy rushes under normal water level conditions, steep angles show strong responses caused by the double-bounce effect, whereas shallower angles show considerable signal attenuation due to volume scattering. In the case of flooded scenes, and given that rushes are covered by water, forward scattering occurs in S1, as well as in S4 and S6 beams. Nevertheless, for certain environmental conditions and incidence angles the radar response enables landscape element discrimination. This is evident in the S6 beam for healthy and burned rushes (Figure 9a).

Figure 9 also addresses the behaviour of radar response from forest non-flooded (Figure 9b) and flooded (Figure 9c). The behaviour is also shown in Figure 10 through the multi-temporal multi-angle profile of forest radar backscatter. It can be observed that flood conditions constitute a critical factor affecting the radar signal that limits the influence of incidence angles.

For non-flooded forest (willow and poplar) the radar response remains stable independently of incidence angle and phenology. In the case of flooded forests, the largest differences in radar

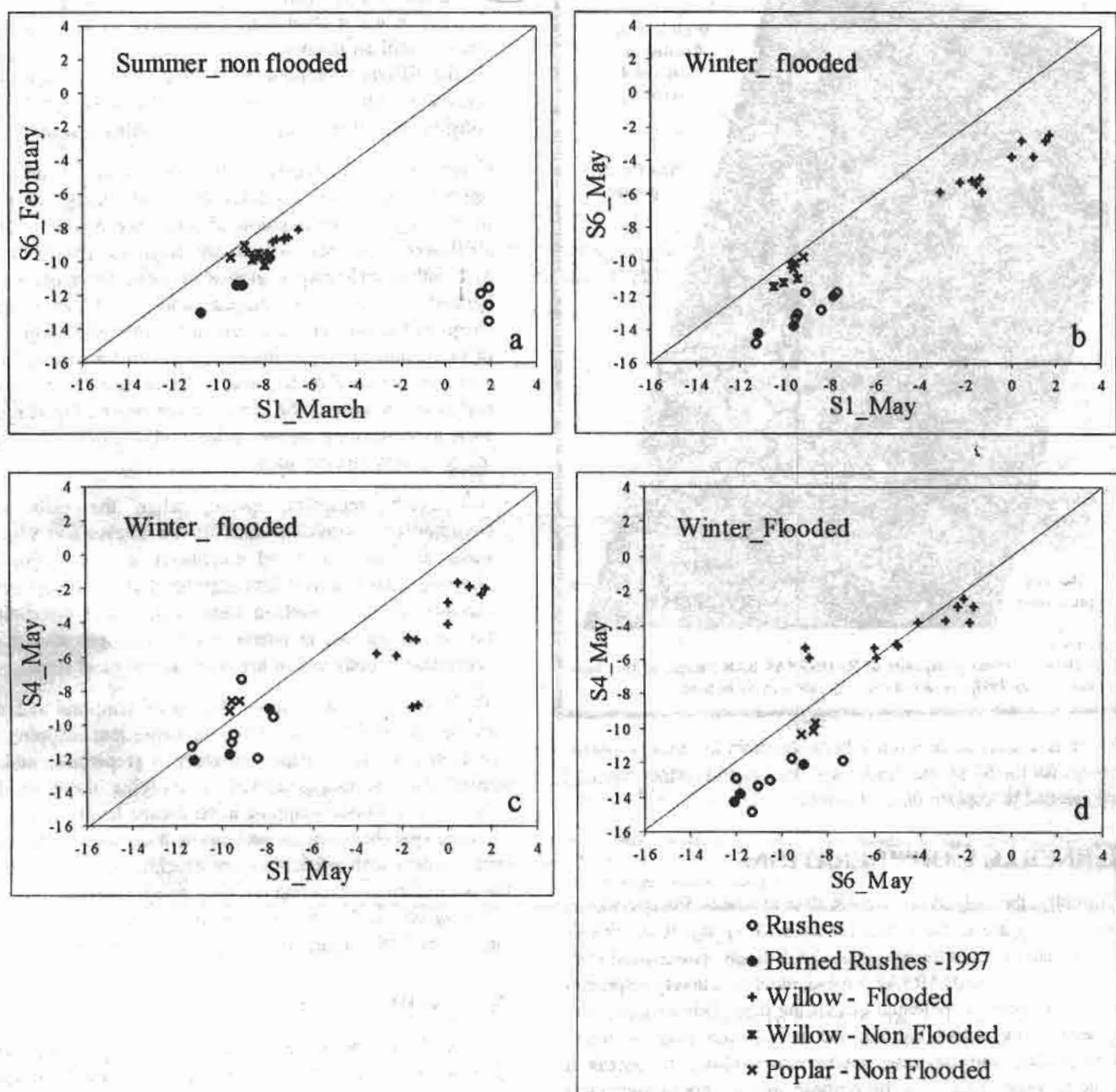


Figure 7.

Scatterplots of measured RADARSAT SAR backscatter values from polygons of two main landscape elements comparing different incidence angles. For late summer, normal condition: a) S6 vs. S1. For winter flooded: b) S6 vs. S1, c) S4 vs. S1, and d) S4 vs. S6.

response are noticed between flooded/non-flooded scenes. Differences due to the incidence angle are less pronounced.

For scenes imaged under normal conditions, differences between young and adult plantations are less than 2 dB, whereas in flooded scenes, differences do not exceed 3 dB. These results are consistent with those published by other authors for multi-temporal C-band ERS-2 observations reported for mature forests (Quegan *et al.*, 2000).

Old and young flooded plantations follow the same trend, but the difference between S1 and S4 is larger for the older

ones (5 dB and 3 dB, respectively). In the case of burned and flooded willow plantations, instead, the pattern is slightly different since the backscattered signal seems to decrease linearly with increasing incidence angle.

When differences between flooded and normal condition scenes are analyzed, young forests show a 6 dB difference and adult forests a 10 dB difference. This might be explained by the difference in the intensity of the trunk-surface contribution to the total  $\sigma^0$ . It is also important to note that burned plantations have a multi-temporal pattern similar to that of healthy ones.



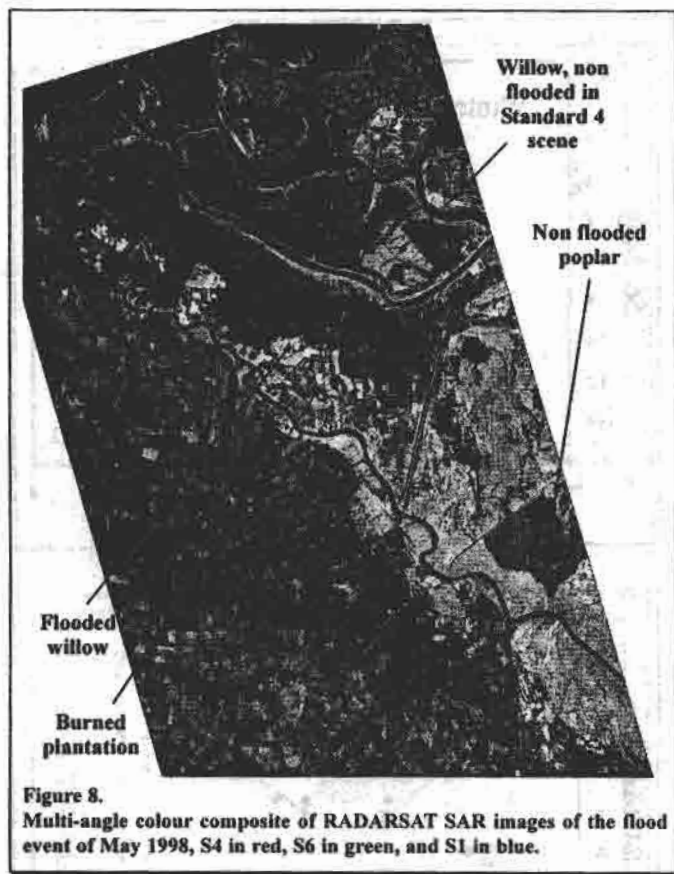


Figure 8.  
Multi-angle colour composite of RADARSAT SAR images of the flood event of May 1998, S4 in red, S6 in green, and S1 in blue.

There is almost no difference between them in radar response, except for the S4 image. Additional images and further research are needed to explain this behaviour.

## GENERAL CONSIDERATIONS

Currently, the only type of SAR data available for operational applications are C-band data for ERS (VV) and RADARSAT (HH) systems. Even though improved data sets are expected from ENVISAT and RADARSAT 2 missions, it is still very important to fully exploit the potential of existing data. This requires both understanding where the relevant information may be found among data and devising appropriate methods to access it (Quegan *et al.*, 2000). For this purpose, multi-temporal signatures are particularly important for many applications. Accordingly, this paper discusses the contribution of multi-temporal multi-angle RADARSAT SAR data to wetland ecosystem monitoring and mapping. The procedure applied was based on the quantitative analysis of the mean backscattering coefficient for samples of well-known sites obtained from images under different environmental conditions and beam modes.

From these results, some general considerations may be drawn:

- Examination of the temporal variability of radar response in wetlands shows that changes in flood condition strongly affect C-HH radar backscatter in forest and rushes. This is evidenced through changes in dominant signal-target

interaction mechanisms. However, since only significant changes in water level were considered in this paper, it remains still an unanswered question, that is, how sensitive are the different components of the backscatter coefficient to regular variations in water level (Richards, 1987b). This constitutes an interesting subject for further research.

- Combinations of images of different incidence angles may improve information extracted from radar images. For flood monitoring the combination of incidence angles is crucial: shallower incidence angles are required for open water delineation, and steep angles are needed for mapping water beneath the forest or vegetation canopy. The combination of steep, and shallower incidence angles may also help in areas of confusion in single images (between burned rushes and forest in the case of S1, and between burned and standing rushes in the case of S6), but further processing is required, such as generating image ratios and/or differences, and/or using decision-based rules.
- As already remarked above, when the influence of environmental conditions such as water level and vegetation status are assessed, flood conditions are the major factor affecting radar returns at landscape level. It constitutes the major variable for radar wetland identification and discrimination because of the strong interaction mechanisms among water and vegetation (woody and/or herbaceous) and radar signal.

These overall results show that multi-temporal radar data may be successfully used for monitoring and mapping flood events in wetlands. A paper currently in preparation addresses classification strategies aimed at applying these results to vegetation and flood mapping at landscape level.

Future spaceborne radar systems will certainly constitute an improvement with respect to current techniques, since they offer the possibility of obtaining not only multi-temporal multi-angle radar signatures, but also polarimetric data which can provide significant information about target structural characteristics.

## ACKNOWLEDGEMENTS

This work has been carried out within the framework of the GlobeSAR-2 project "Suitability of RADARSAT Images for Mapping Forested Areas and Natural Vegetation". This research was funded by the Consejo Nacional de Investigaciones Científicas y Técnicas (CONICET) PID 0646/98, University of Buenos Aires and FonCyT/SECyT PICT Ns. 4503, 1417.

The authors express their gratitude to the members of CONAE's staff who were responsible for coordinating the GlobeSAR-2 Program in Argentina. They are also indebted to CCRS and RADARSAT for providing data and support, and to Dr. Phil Howarth for many useful comments on the manuscript.

## REFERENCES

- Adam, S., Wiebe, J., Collins, M., and Pietroniro, A. (1998). "RADARSAT Flood Mapping in the Peace-Athabasca Delta, Canada". *Canadian Journal of Remote Sensing*, Vol. 24, No. 1, pp. 69-79.

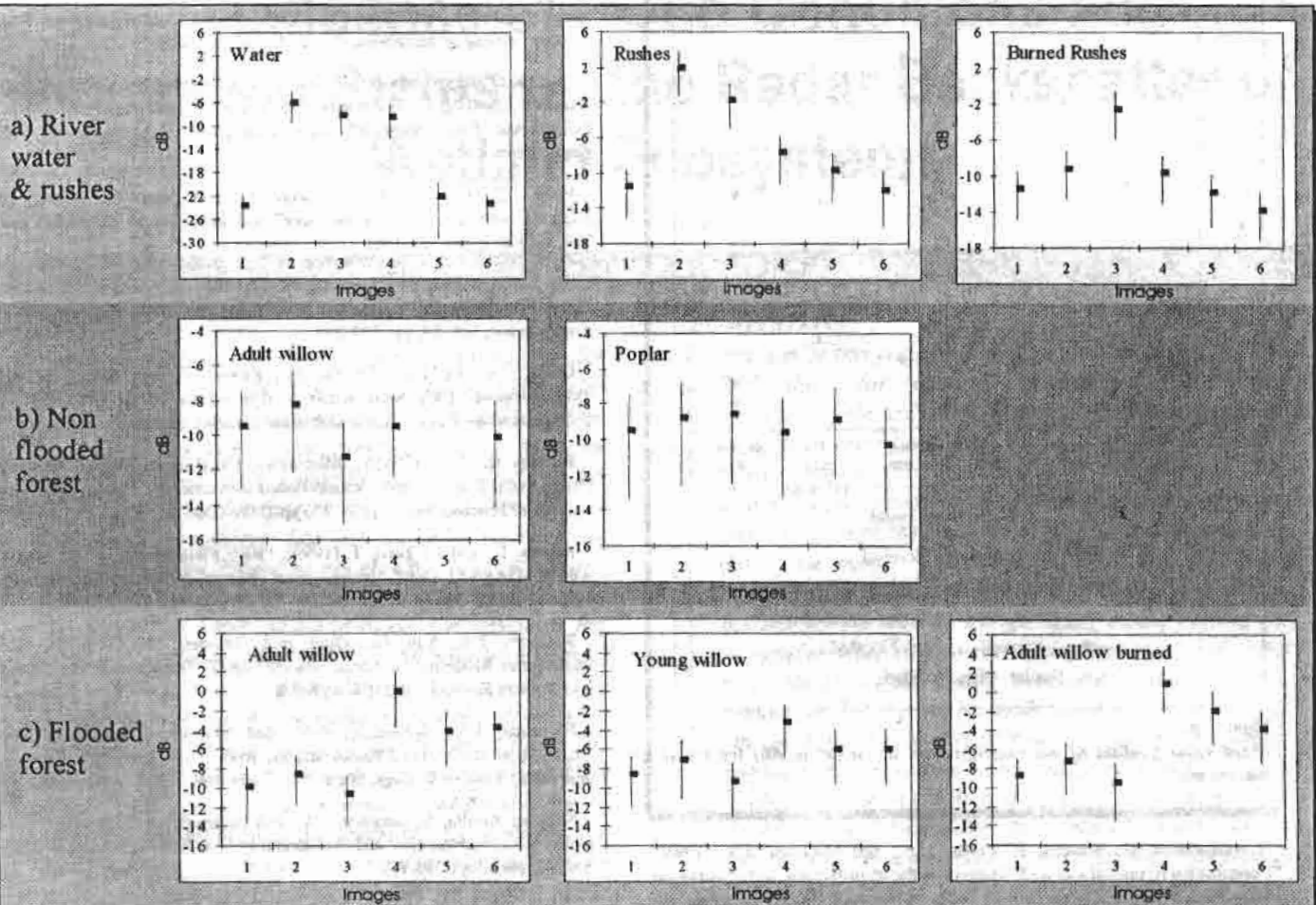


Figure 9.

Mean and Standard Deviation of backscatter values for different land covers: a) River water & rushes, b) Non-flooded forest and c) Flooded forest. Numbers in the abscissa indicate image dates and beams: 1) February 16, 1997/S6; 2) March, 16, 1997/S1; 3) August 7, 1997/S1; 4) May 22, 1998/S1; 5) May 1, 1998/S4; 6) May 18, 1998/S6, (the last three are shown in order of increasing incidence angle).

Beaudoin, A., Le Toan, T., Goze, S., Nezry, E., E. Lopez, A., and Mougin, E. (1994). "Retrieval of Forest Biomass from SAR Data". *International Journal of Remote Sensing*, Vol. 15, No. 14, pp. 2777-2796.

Cihlar, J., Pultz, T.J., and Gray, A.L. (1992). "Change Detection with Synthetic Aperture Radar". *International Journal of Remote Sensing*, Vol. 13, No. 3, pp. 401-414.

Crevier, Y., and Pultz, T.J. (1996). "Analysis of C-Band SIR-C Radar Backscatter over a Flooded Environment, Red River, Manitoba". *Applications of Remote Sensing in Hydrology. Proceedings of the Third International Workshop NHRI Symposium*, No. 17, 47-60. NASA, Goddard Space Flight Center, Greenbelt, Maryland, U.S.A.

Dobson, M.C., Ulaby, F.T., and Pierce, L.E. (1995). "Land-Cover Classification and Estimation of Terrain Attributes Using Synthetic Aperture Radar". *Remote Sensing of Environment*, Vol. 51, pp. 199-214.

Frulla, L.A., Milovich, J.A., Karszenbaum, H., and Kandus, P. (1998). "Metodologías de pre-procesamiento y procesamiento utilizadas en el tratamiento cuantitativo de datos SAR para el estudio de ambientes en el Bajo Delta del Río Paraná, Argentina". *Image Processing Techniques*, (ESA SP-434): 165-174.

Hess L.L., Melack, J.M., Filoso, S., and Wang, Y. (1995). "Delineation of Inundated Area and Vegetation along the Amazon Floodplain with the SIR-C Synthetic Aperture Radar". *IEEE Transactions on Geoscience and Remote Sensing*, Vol. 33, No. 4, pp. 896-903.

Hess, L.L., Melack, J.M., and Simonett, D.S. (1990). "Radar Detection of Flooding Beneath the Forest Canopy: A Review". *International Journal of Remote Sensing*, Vol. 11, No. 7, pp. 1313-1325.

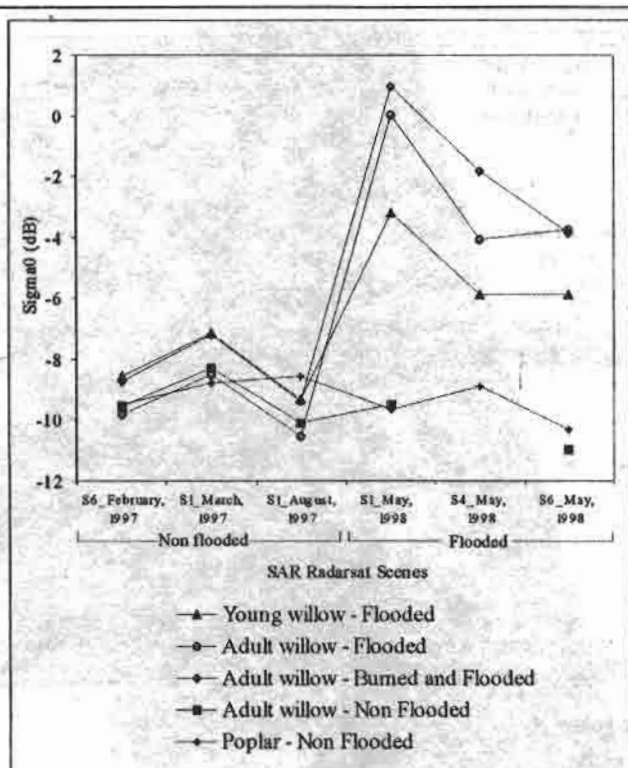
Iriondo, M., and Scotta, E. (1979). "The evolution of the Paraná River Delta". *Proceedings of the 1978 International Symposium on Coastal Evolution in the Quaternary*. Sao Paulo, Brasil, pp. 405-418.

Jensen, J.R. (1993). "An Evaluation of the Coast Watch Change Detection Protocol in South Carolina". *Photogrammetric Engineering and Remote Sensing*, Vol. 53, No. 5, pp. 521-529.

Kandus, P., Karszenbaum, H., and Frulla, L.A. (1999a). "Land cover classification system for the Lower Delta of the Paraná River (Argentina): Its relationship with Landsat Thematic Mapper spectral classes". *Journal of Coastal Research*, Vol. 15, No. 4, pp. 909-926.

Kandus, P. (1997). "Análisis de Patrones de vegetación a escala regional en el Bajo Delta del Río Paraná (Argentina)". *Ph.D. Thesis Dissertation*. Buenos Aires University, Argentina, 200 pp.

Karszenbaum, H., Kandus, P., Parmuchi, G., and Bava, J. (1999). "Evaluation of the effects of El Niño 98 in the Lower Delta Islands of Parana River using RADARSAT images and GIS tools". *GlobeSAR-2 Final Symposium "RADARSAT Applications in Latin America"*, Buenos Aires, Argentina, pp. 240-245.



**Figure 10.**  
Mean value profiles of the backscattered signal ( $\sigma^\circ$  in dB) for forest plantations.

Karszenbaum, H., Kandus, P., Frulla, L.A., and Milovich, J.A. (1998). "Contribution of optical and SAR imagery in the identification and distribution of land cover features in the Lower Delta of Paraná's River, Argentina". In *Proceedings of the International Geoscience and Remote Sensing Symposium*. Seattle, Washington, USA, 6-10 July. IEEE Catalog No. 98CH36174.

Kasischke, E.S., Melack, J.M., and Dobson, M.C. (1997a). "The Use of Imaging Radars for Ecological Applications - A Review". *Remote Sensing of Environment*, Vol. 59, pp. 141-156.

Kasischke, E.S., and Bourgeau-Chavez, L.L. (1997b). "Monitoring South Florida Wetlands Using ERS-1 SAR Imagery". *Photogrammetric Engineering & Remote Sensing*, Vol. 63, No.3, pp. 281-291.

Milovich, J.A., Frulla, L.A., Karszenbaum, H., Kandus, P. and Ross, S. (2000). "Procedures for Utilization of RADARSAT Standard Mode Path Images". Submitted to *Remote Sensing of Environment*.

Noernberg, M.A., Novo, E.M., and Krug, T. (1999). "The Use of Biophysical Indices and Coefficient of Variation Derived from Airborne Synthetic Aperture Radar for Monitoring the Spread of Aquatic Vegetation in Tropical Reservoirs". *International Journal of Remote Sensing*, Vol. 20, No. 1, pp. 67-82.

Parker, G. and Marcolini, S. (1992). "Geomorfología del Delta del Paraná y su extensión hacia el Río de la Plata". *Revista de la Asociación Geológica Argentina*, Vol. 47, No. 2, pp. 243-249.

Pope, K.O., Rey-Benayas, J.M., and Paris, J.F. (1994). "Radar Remote Sensing of Forest and Wetland Ecosystems in the Central American Tropics". *Remote Sensing of Environment*, Vol. 48, pp. 205-219.

Pope, K.O., Rejmankova, E., Paris, J.F., and Woodruff, R. (1997). "Detecting Seasonal Flooding Cycles in Marshes of the Yucatan Peninsula with SIR-C Polarimetric Radar Imagery". *Remote Sensing of Environment*, Vol. 59, pp. 157-166.

Pultz, T.J., Leconte, R., St-Laurent, L., and Peters, L. (1991). "Flood mapping with airborne SAR imagery". *Canadian Water Resources Journal*, Vol. 16, No. 2, pp. 173-189.

Pultz, T.J., Crevier, Y., Brown, R.J., and Boisvert, J. (1997). "Monitoring Local Environmental Conditions with SIR-C/X-SAR". *Remote Sensing of Environment*, Vol. 59, pp. 248-255.

Quegan, S., Le Toan, T., Yu, J.J., Ribbes, F., and Floury, N. (2000). "Multitemporal ERS SAR Analysis Applied to Forest Mapping". *IEEE Transactions on Geoscience and Remote Sensing*. In press.

Ramsey III, E.W. (1995). "Monitoring Flooding in Coastal Wetlands by Using Radar Imagery and Ground-Based Instruments". *International Journal of Remote Sensing*, Vol. 16, No. 13, pp. 2495-2502.

Ribbes, F., and Le Toan, T. (1999). "Rice Field Mapping and Monitoring with RADARSAT Data". *International Journal of Remote Sensing*, Vol. 20, No. 4, pp. 745-765.

Richards, J.A., Sun, Guo-Qing, and Simonett, D.S. (1987a). "L-Band Backscatter Modeling of Forest Stands". *IEEE Transactions on Geoscience and Remote Sensing*, GE25; 4: 487-498.

Richards, J.A., Woodgate, P.W., and Skidmore, A.K. (1987b). "An Explanation of Enhanced Backscattering from Flooded Forest". *International Journal of Remote Sensing*, Vol. 8, No. 7, pp. 1093-1100.

Sanchez-Arcilla, A., Jimenez, J.A., and Valdemoro, H.I. (1998). "The Ebro Delta: Morphodynamics and Vulnerability". *Journal of Coastal Research*, Vol. 14, No.3, pp. 754-772.

Tandis, F.J., Bourgeau Chavez, L.L., and Dobson, M.C. (1994). "Applications of ERS-1 SAR for Coastal Inundation". In *Proceedings of the International Geoscience and Remote Sensing Symposium*. Pasadena, California, 8-12 August. IEEE Catalog No. 94CH3378-7, IEEE New York, pp. 1481-1483.

Wang, Y., and Day, J. (1993). "Santa Barbara Microwave Backscattering Model for Woodlands". *International Journal of Remote Sensing*, Vol. 14, No. 8, pp. 1477-1493.

Wang, Y., Kasischke, E. S., Melack, J. M., Davis, F. W., and Christensen, Jr., N.L. (1994). "The Effects of Changes in Loblolly Pine Biomass and Soil Moisture on ERS-1 SAR Backscatter". *Remote Sensing of Environment*, Vol. 49, pp. 25-31.

Wang, Y., Hess, L.L., Filoso, S., and Melack, J.M. (1995). "Understanding the Radar Backscattering from Flooded and Nonflooded Amazonian Forests: Results from Canopy Backscatter Modeling". *Remote Sensing of Environment*, Vol. 54, pp. 324-332.

Wright, L.D. (1985). "River Deltas". In R.A. Davis (Ed.), *Coastal Sedimentary Environments*, Springer, New York, USA, pp. 1-76.